Impact of Positional Isomers on the Selective Isolation of cis-trans Isomers in Cobaltdioxolene Chemistry and Solvation Effects on the Valence Tautomerism in the Solid State

Narayan Ch Jana, Xing-Hui Qi, Paula Brandão, Corine Mathonière, Anangamohan Panja

Impact of Positional Isomers on the Selective Isolation of *cis-trans* Isomers in Cobalt-dioxolene Chemistry and Solvation Effects on the Valence Tautomerism in the Solid State

Narayan Ch. Jana,[a] *Xing-Hui Qi,*[b] *Paula Brandão,*[c] *Corine Mathonière,**[b,d] *and Anangamohan Panja**[a,e]

[a] *Department of Chemistry, Panskura Banamali College, Panskura RS, WB 721152, India. E-mail: ampanja@yahoo.co.in*

[b] *Univ. Bordeaux, CNRS, Bordeaux INP, ICMCB, UMR 5026, F-33600 Pessac, France. E-mail: corine.mathoniere@u-bordeaux.fr*

[c] *Department of Chemistry, CICECO-Aveiro Institute of Materials, University of Aveiro, 3810-193 Aveiro, Portugal*

[d] *Univ. Bordeaux, CNRS, Centre de Recherche Paul Pascal, CRPP, UMR 5031, F-33600 Pessac, France. E-mail: corine.mathoniere@u-bordeaux.fr*

[e] *Department of Chemistry, Gokhale Memorial Girls' College, 1/1 Harish Mukherjee Road, Kolkata-700020, India*

ABSTRACT: Three new mononuclear cobalt compounds, *trans*-[Co(3,5-dbcat)(3,5-dbsq)(4-Etpy)$_2$]·CH_3CN (**1**), *cis*-[Co(3,5-dbcat)(3,5-dbsq)(3-NH_2py)$_2$]·DMF (**2**) and *trans*-[Co(3,5-dbcat)(3,5-dbsq)(4-NH_2py)$_2$]·2DMF (**3**) (3,5-dbcat^{2-} and 3,5-dbsq$^{\bullet-}$ stand for 3,5-di-*tert*-butyl-catacholate and 3,5-di-*tert*-butyl-semiquinonate, respectively), derived from a redox-active *o*-dioxolene ligand in presence of 4-ethylpyridine (4-Etpy), 3-aminopyridine (3-NH_2py), and 4-aminopyridine (4-NH_2py), respectively, have been synthesized and investigated with a view to examine possible influence of pyridine derivatives and solvation on the valence tautomeric (VT) process. Single crystal X-ray diffraction data for all compounds at room temperature suggest Co(III)(3,5-dbcat)(3,5-dbsq) charge distribution in these complexes. Further insight into the crystal structures discloses the diverse noncovalent interactions offered by the isomers of aminopyridine in **2** and **3**, leading to the first example

of selective isolation of *cis* and *trans* isomers in cobalt-dioxolene chemistry induced by the positional isomers of the ancillary ligands. Variable temperature magnetic susceptibility data for all compounds between 2 and 300 K are consistent with the structural studies. At elevated temperatures, complex **1** exhibits a VT interconversion from low spin Co(III)-(3,5-dbcat)(3,5-dbsq) to high spin Co(II)-(3,5-dbsq)(3,5-dbsq), triggered by the loss of lattice solvent molecules, while a partial interconversion is observed for complex **3** even heating up to 430 K. The present report overall highlights the impact of positional isomers on the selective isolation of *cis*-*trans* isomers in cobalt-dioxolene chemistry and solvation effects on the valence tautomerism in the solid state.

INTRODUCTION

The molecular materials that can be reversibly switched between distinguishable states, are of great interest in the scientific community. The molecular switchable compounds are particularly attractive because of the feasibility of fine-tuning in the chemical architecture which allows tailor-made applications, such as sensors, information storage devices, or in the field of molecular electronics.[1–10] Molecule-based systems that exhibit an intramolecular electron transfer (IET) phenomenon can be switched between isomers with different electronic states.[11–17] Valence tautomerism is also a specific phenomenon that involves a stimulated and reversible intramolecular electron transfer between a transition metal and a redox-active ligand.[18–20] Octahedral cobalt complexes with redox non-innocent dioxolene ligand are so far the most popular family of valence tautomeric (VT) complexes particularly those involves 3,5-di-*tert*-butyl-dioxolene (3,5-dbdiox) and nitrogen-donor ancillary ligands.[21–33] In these systems, an intramolecular electron transfer occurs between two redox isomers that exhibit low-spin (ls) Co(III)-catecholate (cat^{2-}) at low temperature, while the high-spin (hs) Co(II)-semiquinonate ($sq^{\bullet-}$) state is favored at higher temperatures.[11,34] Thermally and optically induced VT transitions are the most common, while influence of pressure,[35] soft X-ray[36–38] and magnetic field[39] on VT transitions have also been reported but in less extent.

After the discovery of the first VT cobalt-dioxolene complex,[40] [Co(III)(3,5-dbcat)(3,5-dbsq)(2,2′-bpy)] (where 2,2′-bpy is 2,2′-bipyridine), most of the other VT bis(*o*-dioxolene)cobalt complexes have been reported by replacing 2,2′-bpy ligand with other bidentate N,N-donor ancillary ligands. Such complexes always adopt the *cis* orientation of the N-donor atoms due to the structural restraints. By employing monodentate N-donor

ligands in place of bidentate N-donor ligands, the *trans* arrangement of the ancillary ligands can be achieved and several such reports are available in the literature.[41–43] Most of these complexes exhibit VT transitions in the solid state where intermolecular interactions between the chemical moieties, packing effect and solvent effect influence the characteristics of the electronic transition, inducing abruptness and bistability/hysteresis that will enable application in devices. In this regard, Shultz et al. used different derivatives of monodentate pyridyl N-donor ligand to coordinate [Co(3,5-dbdiox)$_2$] units, which ultimately resulted *trans* isomer in all the cases.[41,42] More recently, Boskovic et al. reported *trans* form of different solvated VT complexes using 3,5-dbdiox and pyridine ligand.[43] Recently, we have explored how the crystal packing governed by different kinds of noncovalent forces affects the valence tautomeric equilibrium in cobalt-dioxolene system.[44] Moreover, we successfully isolated both *cis* and *trans* isomers for the first time in cobalt-dioxolene chemistry and found the crucial role of the solvent polarity in the isolation of these isomers. We have also realized that although the energetics of *cis* and *trans* isomers are comparable, the non-covalent interaction in the solid state played an important role for isolation of the isomeric compounds. Apart from that these geometrical differences, different orientations of the ligand-based magnetic orbitals in these isomers may bring distinct electronic properties and hence influences the VT phenomenon. Therefore, it still remains a challenge to synthesize such isomeric compounds in the cobalt-dioxolene chemistry.

As a part of our ongoing research on the transition metal dioxolene chemistry,[44–52] here we aim to develop dioxolene-based complexes with varied geometrical isomers around the metal center by suitable choice of solvent and/or different N-donor ligands. As it has been realized from our previous report, role of the noncovalent interactions in isolation of the geometrical isomers in cobalt-dioxolene chemistry, introduction of the positional isomers of the pyridine derivative may bring different noncovalent interactions, leading to isolation of different products.[44] Therefore, in the present work, we employed two positional isomers of aminopyridine, where the pendent amine group has a potential to establish at least hydrogen bonding interaction in different directions in the solid state. Accordingly, herein, we report the synthesis and structural characterization of three new mononuclear cobalt compounds, *trans*-[Co(3,5-dbcat)(3,5-dbsq)(4-Etpy)$_2$]·CH_3CN (**1**), *cis*-[Co(3,5-dbcat)(3,5-dbsq)(3-NH_2py)$_2$]·DMF (**2**) and *trans*-[Co(3,5-dbcat)(3,5-dbsq)(4-NH_2py)$_2$]·2DMF (**3**) derived from 3,5-dbdiox (3,5-dbcat^{2-} and 3,5-dbsq$^{\bullet-}$ stand for 3,5-di-*tert*-butyl-catacholate and 3,5-di-*tert*-butyl-semiquinonate, respectively) in presence of 4-ethylpyridine (4-Etpy), 3-aminopyridine (3-NH_2py), and 4-aminopyridine (4-NH_2py), respectively (Scheme 1). The VT behavior of

these complexes and the influence of positional isomers of the ancillary ligands on the isolation of different geometrical isomers have been explored.

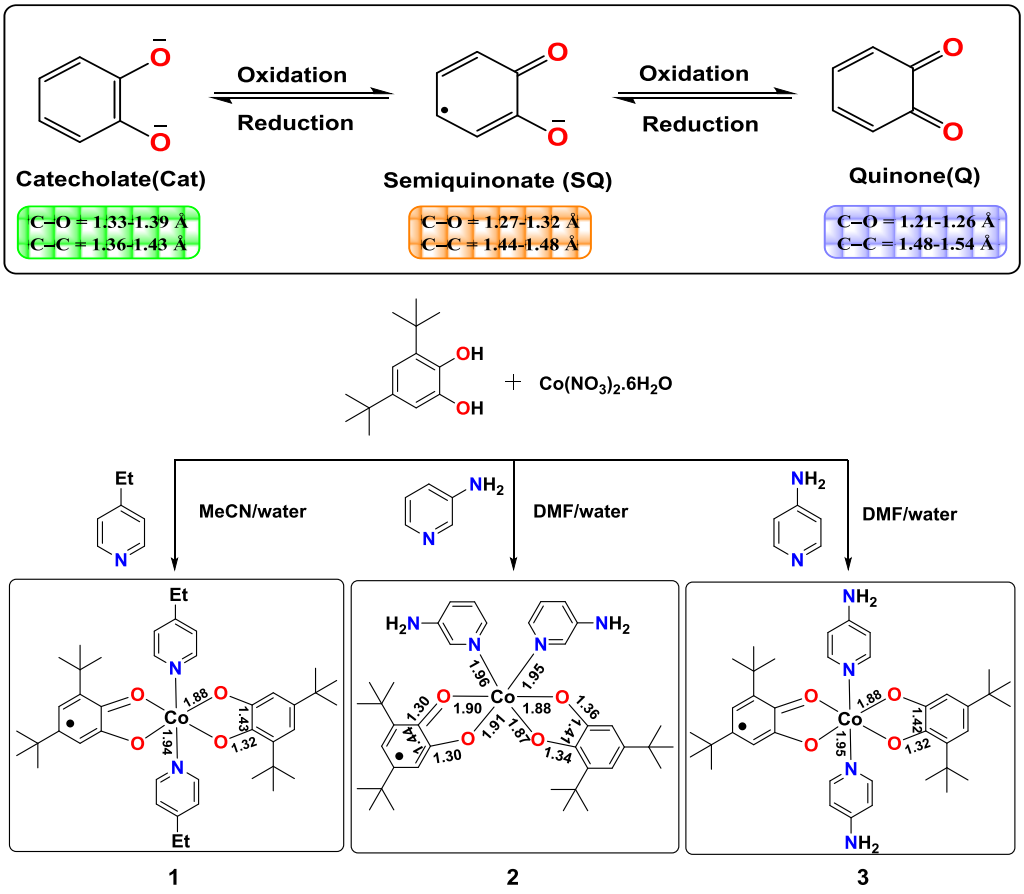

Scheme 1. Possible redox isomers of a dioxolene ligand (top) and the schematic representation of the synthetic routes to **1-3** and the crystallographic bond distances (Å) in **1-3**.

EXPERIMENTAL SECTION

Materials and physical methods

Cobalt(II) nitrate hexahydrate was purchased from commercial sources and was used as received. 3,5-di-*tert*-butyl-catechol (3,5-H_2dbcat) and 4-Ethylpyridine were purchased from Sigma-Aldrich. 3-aminopyridne and 4-aminopyridine were purchased from SRL Pvt. Ltd., India. Solvents were of analytical grade and used without further purification.

Elemental analyses (C, H, N) were performed by Perkin–Elmer 240C elemental analyzer. IR spectra of all the complexes at room temperature and **1** after heating at 380 K followed by

cooling the sample back to room temperature were measured using a Thermo Scientific Nicolet iS5 FTIR spectrometer with a universal ATR sampling accessory from 4000 to 400 cm^{-1}. An Agilent Diode array spectrophotometer (Agilent Carry 60) with a 1-cm-path-length quartz-cell was used to record absorption spectra of the samples. The thermogravimetric analyses (TGA) were performed on a Perkin-15 Elmer Pyris Diamond TGA/DTA analyzer in a dynamic nitrogen atmosphere with a heating rate of 5°C min^{-1}. The X-band EPR spectra of as synthesized complex **1-3** and after desolvation (for **1)** were measured in the solid state using a JEOL JES-FA 200 instrument at room temperature. Room temperature powder X-ray diffraction (PXRD) measurements were carried out using a Rigaku Smart Lab X-ray diffractometer with a Cu-Kα source.

Synthesis of *trans*-[Co(3,5-dbcat)(3,5-dbsq)(4-Etpy)$_2$]·CH$_3$CN (1). All manipulations were carried out under aerobic condition for the synthesis of all three complexes. An aqueous solution (2 mL) of $Co(NO_3)_2·6H_2O$ (0.072 g, 0.25 mmol) was added to an acetonitrile solution (10 mL) of 3,5-H_2dbcat (0.111 g, 0.5 mmol) and 4-ethylpyridine (4-Etpy) (0.107 g, 1 mmol) with stirring and the resulted solution was filtered and kept at ambient temperature for crystallization. Dark green crystals of **1** suitable for single-crystal X-ray diffraction were obtained in two days. Yield: 0.155 g (82%). Anal. Calcd. for $C_{44}H_{61}CoN_3O_4$: C, 70.01; H, 8.14; N, 5.57. Found: C, 69.85; H, 7.89; N, 5.42 IR (cm^{-1}): 2954w, 1617s, 1574m, 1478m, 1457m, 1389s, 1282s, 1247m, 1208m, 1068m, 984m, 900m, 685w, 542m.

Synthesis of *cis*-[Co(3,5-dbcat)(3,5-dbsq)(3-NH$_2$py)$_2$]·DMF (2). Complex **2** was synthesized from DMF/water (5:1 v/v) mixture by adopting a very similar method as that employed for **1** but 3-aminopyridine was used instead of 4-ethylpyridine. The dark-blue block-crystals suitable for X-ray diffraction were obtained from the reaction mixture upon standing at ambient temperature within a couple of days. Yield: 0.162 g (85%). Anal Calcd. for $C_{41}H_{59}CoN_5O_5$: C, 64.72; H, 7.82; N, 9.20. Found: C, 64.55; H, 7.59; N, 9.05. IR (cm^{-1}): 3445br, 3333s, 3210w, 2954s, 1660m, 1617m, 1602m, 1580s, 1437s, 1382s, 1280m, 1193m, 1058m, 1021m, 975m, 909m, 829m, 804m, 698m, 602m, 518m.

Syntheses of *trans*-[Co(3,5-dbcat)(3,5-dbsq)(4-NH$_2$py)$_2$]·2DMF (3). Complex **3** was synthesized from DMF/water (5:1 v/v) mixture following the same methodology as that applied for the synthesis of **1** but 4-aminopyridine was used in place of 4-ethylpyridine. Green plate shaped crystals suitable for X-ray crystallography were obtained within a couple of days. Yield: 0.165 g (79%). Anal Calcd. for $C_{44}H_{67}CoN_6O_6$: C, 63.29; H, 8.09; N, 10.07.

Found: C, 63.25; H, 8.05; N, 10.03. IR (cm^{-1}, KBr): 3429br, 3321m, 2944w, 1668s, 1633m, 1517m, 1456m, 1381m, 1278m, 1203s, 1089m, 1058m, 984m, 850m, 680m, 542m, 487s.

X-ray Crystallography

Single crystal X-ray diffraction measurements of the complexes were made on a Bruker Smart Apex-II CCD diffractometer with monochromated Mo-Kα radiation (λ = 0.71073 Å) at room temperature. Several scans in φ and ω directions were made to increase the number of redundant reflections and were averaged during refinement cycles. Bruker APEX-II suite (v2.0-2) program was used for data collection, data reduction, structure solution and refinement. Reflections were then corrected for absorption, inter frame scaling and other systematic errors with SADABS programme.[53] The structures were solved using direct methods within SHELXS and the refinement of the structures was carried out using a least squares method based on F^2 with SHELXL-2013.[54] Anisotropic thermal parameters were applied to refine all the non-hydrogen atoms. Hydrogen atoms attached to carbon were placed at geometrically idealized positions with individual isotropic thermal factors equal to 1.2 and 1.5 times of those to which they are attached. Hydrogen atoms attached to nitrogen atoms (N39 and N46 from complex **2** and N23 from complex **3**) were located on the difference Fourier map and isotropically treated. The detailed crystallographic data together with refinement details are presented in Table 1.

Magnetometry

Magnetic susceptibility measurements were performed on a Quantum Design MPMS-XL SQUID magnetometer working at temperatures between 1.8 K and 380 K and *dc* magnetic field ranging from -7 and +7 T and on a Microsense VSM (Vibrating Sample Magnetometer) EZ7 working at temperatures between 100 K and 1000 K and *dc* magnetic field ranging from -1.8 and +1.8 T. The polycrystalline samples for SQUID (m = 23.36 mg for **1,** m = 8.94 mg for **2** and m = 7.43 mg for **3**) are introduced in a sealed polypropylene bag and for VSM ((m = 9.2 mg for **1**) are introduced in quartz capsule. Experimental data were corrected for sample holder and intrinsic diamagnetic contributions.

Table 1. Crystal data and structure refinement for complexes **1–3**.

	1	**2**	**3**
Empirical formula	$C_{44}H_{61}CoN_3O_4$	$C_{41}H_{59}CoN_5O_5$	$C_{44}H_{67}CoN_6O_6$
Formula weight (g mol^{-1})	754.88	760.86	834.96
Temperature (K)	296(2)	296(2)	296(2)
Crystal system	Triclinic	Monoclinic	Monoclinic
Space group	$P\bar{1}$	$P2_1/c$	$C2/c$
a (Å)	11.4691(8)	20.9601(8)	25.039(4)
b (Å)	13.5716(9)	11.4324(5)	14.808(2)
c (Å)	15.9489(12)	18.2796(9)	15.708(3)
α (°)	66.057(3)	90	90
β (°)	72.922(3)	105.6495(16)	127.164(4)
γ (°)	87.357(3)	90	90
volume (Å^3)	2161.2(3)	4217.9(3)	4641.1(13)
Z	2	4	4
D_{calc} (mg m^{-3})	1.487	1.198	1.195
μ (mm^{-1})	0.975	0.453	0.420
F (000)	810	1628	1792
θ Range (°)	2.285–25.242	2.214–25.380	2.594–29.246
Reflections collected	70475	34287	36574
Independent reflections (R_{int})	9661(0.0361)	7696(0.0534)	6283(0.0334)
Observed reflections [I≥2σ(I)]	7681	5677	4962
Restraints/parameters	0/487	4/499	2/275
Goodness-of-fit on F^2	1.026	1.025	1.041
Final R indices [I≥2σ(I)]	R_1 = 0.0435 wR_2 = 0.1136	R_1 = 0.0430 wR_2 = 0.1050	R_1 = 0.0413 wR_2 = 0.1068
R indices (all data)	R_1 = 0.0589 wR_2 = 0.1255	R_1 = 0.0700 wR_2 = 0.1203	R_1 = 0.0557 wR_2 = 0.1178
Largest diff. peak/hole (e Å^{-3})	0.589/ –0.382	0.374/ –0.314	0.529/ –0.238

Optical reflectivity measurements

The surface reflectivity measurements have been performed with a home-built system, operating between 10 and 300 K and in a spectrometric range from 400–1000 nm. A halogen-tungsten light source (Leica CLS 150 XD tungsten halogen source adjustable from 0.05 mW cm^{-2} to 1 W cm^{-2}) was used as the spectroscopic light. The measurements were calibrated by barium sulphate as reference sample. With this reflectivity technique, we plot the absolute reflectivity (*AR*) at a specific wavelength λ as $AR(\lambda) = (R_{sample}(\lambda) - R_{dark}(\lambda)) / (R_{ref}(\lambda) - R_{dark}(\lambda))$. The corresponding spectra $AR = f(\lambda)$ can be viewed as a mirror image of the absorbance spectra, meaning when the sample absorbs efficiently (or weakly) the light, a low (or high, respectively) value of *AR* is measured. As the samples are potentially photosensitive, the light exposure time was minimized during the experiments keeping the samples in the dark except during the spectra measurements when white light is shined on the sample surface (P = 0.08 mW cm^{-2}). For all the excitation/de-excitation experiments performed at 10 K, the sample was initially placed at this temperature keeping the sample in the dark to avoid any excitation. Heating and cooling measurements were carried out at 4 K min^{-1}. For white light irradiation, the source described above was used, but in a continuous manner with a power of 0.08 mW cm^{-2}. 14 Light Emitting Diodes (LEDs) from Thorlabs operating at 365 - 385 - 405 - 455 - 505 - 530 - 590 - 625 - 660 - 735 - 780 - 850 - 940 - 1050 nm were used for excitation experiments.

RESULT AND DISCUSSION

Synthesis

An acetonitrile-water (5:1 v/v) mixture of cobalt(II) nitrate hexahydrate, 3,5-di-*tert*-butylcatechol (3,5-H_2dbcat) and 4-ethylpyridine in 1:2:4 molar ratio under aerobic condition resulted in an instantaneous olive-green solution, which upon standing at ambient temperature afforded dark-green crystals of **1** after two days. On the other hand, under a similar reaction condition, a mixture of $Co(NO_3)_2.6H_2O$, 3,5-H_2dbcat and aminopyridines (3-aminopyridine for **2** and 4-aminopyridine for **3**) in a DMF-water (5:1 v/v) mixture led to formation of blue and dark green solutions, which afforded blue block and plate shaped green crystals for **2** and **3**, respectively. In all the cases, the precursor cobalt(II) salt is air-oxidized to cobalt(III) in the presence of the redox active ligand and ancillary pyridyl ligands. Excess amount of pyridines were used to deprotonate 3,5-H_2dbcat ligand and to provide basic

environment for the requirement of oxidation of cobalt(II). Isolation of the crystals and the structure determinations of **2** and **3** ultimately reveal a unique result in this cobalt-dioxolene chemistry where *cis* and *trans* isomers were selectively isolated in reasonable yields by using positional isomers of the ancillary aminopyridyl ligands. 3-aminopyridine resulted a *cis* isomer (**2**) while 4-aminopyridine afforded a *trans* isomer (**3**) under an identical reaction condition. All the complexes are soluble in common organic solvents including acetonitrile and DMF.

UV-vis spectral study

Electronic absorption spectrum of complex **1** was recorded in acetonitrile whereas the spectra of **2** and **3** were measured in DMF solvent to check the nature of the compounds in the solvents from which they synthesized (Figure S1a). UV-vis spectra of **2** and **3** were also recorded in acetonitrile with no noticeable change in electronic transitions (Figure 1, left). UV-vis spectral study proves stability of *cis*-isomer (**2**) over a period of 1 day even at measurable temperature range (Figure S2). UV-vis spectra in different solvents further suggest that both **2** and **3** are thermodynamically controlled products and their formation is not dependent of the solvent polarity (Figure S1b). Here, involvement of the pendant amine groups of aminopyridines in different non-covalent interactions could play important roles behind the selective isolation of *cis* and *trans* isomeric complexes of **2** and **3**, respectively (vide infra). In all the complexes, shoulders/bands at around 580 nm band is associated with the ls-Co(III)-(cat)(sq) tautomer, and the ~770 nm band is characteristic of the hs-Co(II)-$(sq)_2$ tautomer in agreement with the previous studies on similar systems as well as recently reported TD-DFT studies on closely related systems.[22–24,55] The bands at around 400 nm can tentatively be assigned as a ligand-based n−π* transition. The band at around 580 nm is due to the localized semiquinonate π−π* transition in ls-Co(III)-(cat)(sq) tautomer,[55] whereas the bands at around 750 nm may be assigned as the metal-to-ligand charge transfer (MLCT) band from the e_g orbital of Co(II) center to π* orbital of 3,5-$dbsq^{\bullet-}$ in the hs-Co(II)-$(sq)_2$ species. The spectral features nicely agree with the presence of both ls-Co(III)-catecholate and hs-Co(II)-semiquinonate tautomers in solution at room temperature for these compounds.

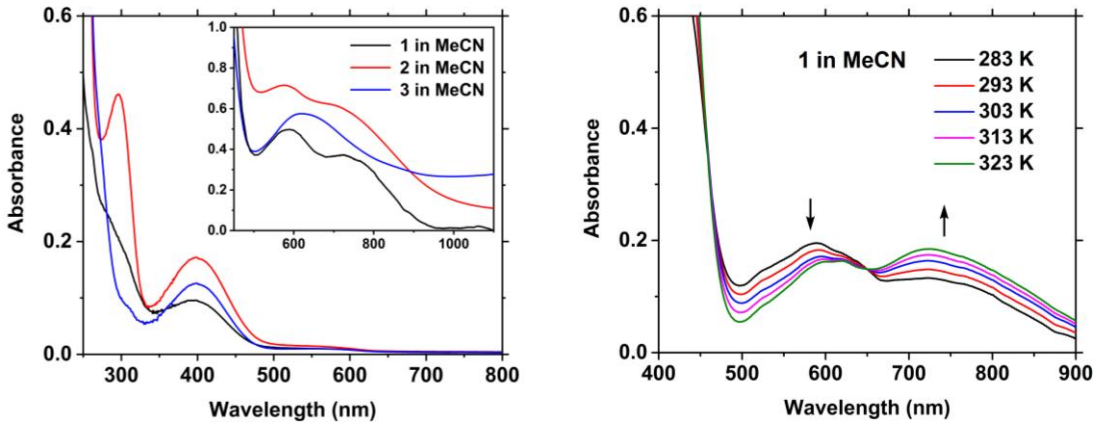

Figure 1: (left) UV-vis spectra of **1–3** in acetonitrile at [complex] = $1x10^{-4}$ M, whereas the inset spectra were recorded at [complex] = $1x10^{-3}$ M and (right) Variable temperature UV-vis spectra of **1** in CH_3CN in the temperature range of 283−323 K.

The variable-temperature UV-vis spectroscopy is known to be a useful tool in probing valence tautomerism, relying on the temperature dependence of absorption bands associated with either the ls-Co(III) or hs-Co(II) isomers. For that variable temperature UV-vis spectra for complex **1** in acetonitrile were recorded in the temperature range 283–323 K (Figure 1, right). The figure shows that as the temperature is increased from 283 K to 323 K, intensity of the band related to ls-Co(III) species at around 580 nm decrease with concomitant increase of intensity of the band at around 750 nm, which indicate the thermal population of [Co^{II}(3,5-dbsq)(3,5-dbsq)(4-Etpy)$_2$] isomer as reported earlier.[41,56] The increase of intensity of the band at 750 nm is associated with the MLCT transition from the e_g orbital of Co(II) center to 3,5-$dbsq^{\bullet-}$ in the high spin Co(II) isomer. Finally, the appearance of isosbestic points at 457 and 650 nm is consistent with the presence of at least two different species, originating from the VT process. Thus complex **1** was found to undergo in solution a thermally induced VT process through an electron transfer from the 3,5-dbcat ligand to Co(III) ion to generate high spin Co(II) isomer.[41,56] Complexes **2** and **3** also exbibit minor changes of the spectral bands in the range 400-800 nm at different temperatures, suggesting that VT process is less active at around room temperature (Figure S3).

IR spectroscopy

The oxidation states of the redox active dioxolene ligands are usually characterized by IR spectroscopy. In the solid state, the C–O stretching modes, such as the intense absorption bands at ca. 1600–1675 cm^{-1} for quinone, ca. 1400–1550 cm^{-1} for semiquinone, and ca. 1250

cm^{-1} for catecholate, are especially useful to distinguish the oxidation states of such ligands. In the IR spectra of these complexes (Figures S4–S6), the bands at *ca*. 1480 cm^{-1} and 1250–1300 cm^{-1} can be assigned to the C−C ring and C−O stretching of the catecholate ligands, respectively, while the bands at around 1440 and 1580 cm^{-1} are characteristic of semiquinonate ligands, consistent with the reported results on similar complexes.[22–25,43,57] A characteristic stretching band associated with the coordinated pyridine molecules are observed in between 450 and 650 cm^{-1}.[43] The IR spectra of all the complexes at room temperature also display bands over the range 2850 to 2960 cm^{-1}, typical for the stretching frequencies of the C−H bond of the *tert*-butyl groups.[43] Based on these IR data, we deduce that each complex contains two *o*-dioxolene forms (i. e. semiquinonate and catecholate) of the ligands at room temperature. These conclusions are confirmed by the EPR spectroscopic studies at room temperature of these samples that reveal the signal of a radical at g = 2.00 (Figure S7), further indicating the existence of a radical species, 3,5-dbsq$^{\bullet-}$, in the solid state.

Structural Study

The neutral complex **1** was isolated from an acetonitrile/water solvent mixture and X-ray structural analysis at 296 K reveals that it crystalized in the triclinic space group $P\bar{1}$ in which the asymmetric unit contains one half of each of two crystallographically independent complex molecules and one solvent acetonitrile molecule. A representative complex molecule along with selected atom numbering scheme is depicted in Figure 2, and important bond distances and bond angles are given in Table 2 and Table S1, respectively. The metal center in each crystallographically independent complex molecule sits on an inversion center and the coordination environments around the metal centers in both complex molecules are eventually identical with general formula [Co(III)(3,5-dbcat)(3,5-dbsq)(4-Etpy)$_2$]. The geometry of the metal centers in these complex molecules can be best described as a slightly distorted octahedral structure being connected with two *o*-dioxolene ligands and two pyridyl groups in *trans* configuration.[41–43] The Co−O and Co−N bond distances of *o*-dioxolene ligands and pyridyl groups, respectively, vary in the ranges 1.8760(13)–1.8849(12) Å and 1.9451(15)−1.9482(19) Å, which are consistent with Co(III) centers in both complex molecules.[41–43,58–63] Measurements of the C−O and (O)C−C(O) bond distances are generally considered to diagnose the oxidation state of *o*-dioxolene ligands. Typical C−O distances for catecholate and semiquinonate ligands are in the range 1.33−1.39 Å and 1.27−1.32 Å, respectively, while ring (O)C−C(O) bond distances vary in the range 1.36−1.43 Å for

catecholate ligand and in the range 1.44−1.48 Å for semiquinonate ligand. The C−O and (O)C−C(O) bond lengths for both independent complex molecules of **1** are in the range 1.315(2)−1.322(2) Å and 1.432(6)−1.435(6) Å, respectively. These values lie in between typical distances for semiquinonate and catecholate ligands, consistent with disorder of the 3,5-dbsq$^{\bullet-}$ and 3,5-dbcat^{2-} redox states of the ligand over the two *o*-dioxolene positions in both complex molecules.[41–43,64–66] The "metrical oxidation state" (MOS) as proposed by Brown[67] was calculated considering all the C−O and C−C bond distances of *o*-dioxolene ligand and found to be –1.46 and –1.50 for two crystallographically independent dioxolene ligands present in the asymmetric unit of **1**, that further supports the intermediate oxidation state of the redox active *o*-dioxolene ligand in these complex molecules. The Bond Valence Sum (BVS) calculations were further performed to determine the oxidation state of cobalt using the following general expression as proposed by Brown and Altermatt:[68] $V_i = \Sigma s_{ij} = \Sigma \exp[(r_0 - r_{ij})/b]$, where r_0 and r_{ij} are empirical and crystallographic bond distances between atoms i and j, respectively; b is the "universal parameter" and is set equal to 0.37; s_{ij} is the valence between atoms i and j; V_i is the sum of all valences s_{ij} of a coordination sphere around the metal ion, and its value is the approximation of the formal oxidation state.[69] The BVS values for two crystallographically independent complex molecules in **1** are calculated to be 3.24–3.26 and 3.24 considering empirical bond distances either of +II or +III oxidation states of cobalt, respectively, further confirming the +III oxidation state of cobalt at room temperature in **1**. From the detailed analysis of the crystal structure, it is found that a T-shape C–H···π interaction is present in the molecule to establish the solid-state stability of the complex (Figure 3). The π···π interaction between the pyridyl ring provides further stability in the solid state (Figure 3).

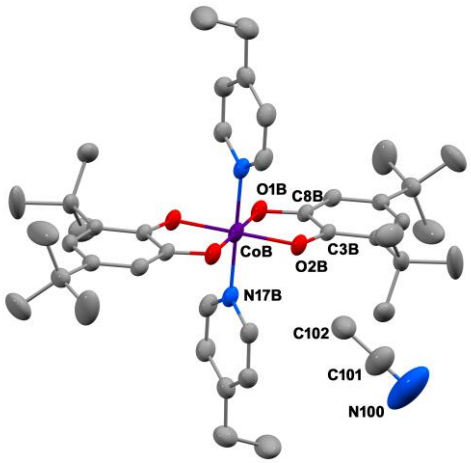

Figure 2. Ellipsoid view of one crystallographically independent molecule and one solvent acetonitrile molecule present in **1** with partial atom numbering scheme. Ellipsoids are drawn at 30% probability. Hydrogen atoms are omitted for clarity.

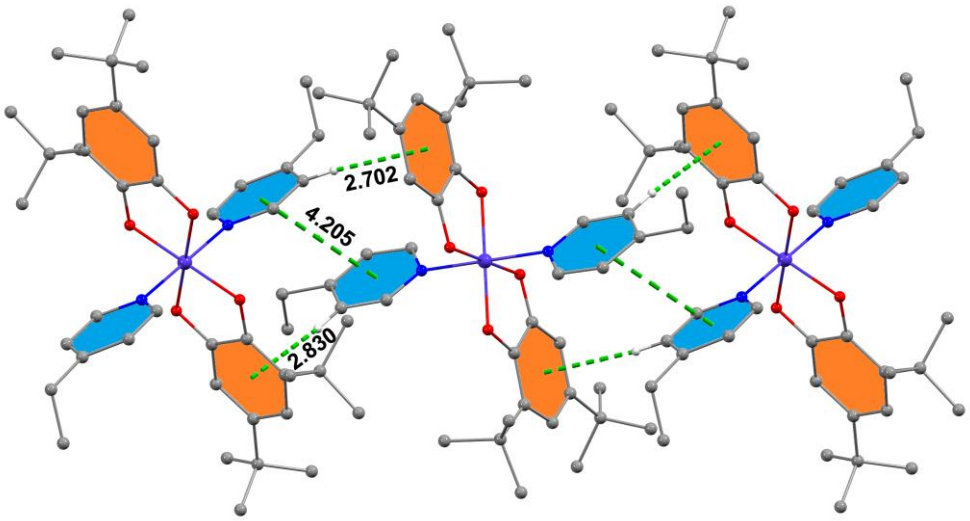

Figure 3: Molecular packing of **1** showing π···π and C–H···π interactions.

Table 2. Selected bond lengths Å and oxidation state parameters for **1**–**3**

	1[a]		**2**	**3**
	A	B		
Co–O (dioxolene)	1.8799(12) 1.8849(12)	1.8795(13) 1.8760(13)	1.9073(17) 1.9042(17) 1.8674(17) 1.8806(16)	1.8835(10) 1.8815(10)
Co–N (pyridine)	1.9451(15)	1.9482(19)	1.950(2) 1.963(2)	1.9493(12)
C–O ($dbsq^{\bullet-}$/$dbcat^{2-}$)	1.322(2) 1.319(2)	1.322(2) 1.315(2)	1.300(3) 1.302(3) 1.357(3) 1.357(3)	1.3215(17) 1.3204(16)
C–C ($dbsq^{\bullet-}$/$dbcat^{2-}$)	1.432(2)	1.435(3)	1.442(3) 1.408(3)	1.4230(19)
MOS[b]	–1.46	–1.50	–1.20 –1.91	–1.50

[a] A and B denote two independent molecules in the asymmetric unit; [b] Metrical Oxidation State

X-ray structural analysis at 296 K shows that both **2** and **3** crystalize in the monoclinic

unit cell with space group $P2_1/c$ and $C2/c$, respectively. The asymmetric unit of complex **2** contains one neutral molecule of [Co(III)(3,5-dbcat)(3,5-dbsq)(3-NH_2py)$_2$] and one DMF solvent, while half of the complex molecule of [Co(III)(3,5-dbcat)(3,5-dbsq)(4-NH_2py)$_2$], sitting on an inversion center, and one DMF molecule are present in the asymmetric unit in **3**. The molecular pictograms along with atom numbering scheme for **2** and **3** are depicted in Figure 4, and the bond parameters can be found in Table 2 and Table S1. The coordination environment around the metal centers is identical with that found in **1** and consists of N_2O_4 donor sites. The geometry of the metal centers in these complexes are again a distorted octahedral structure; however, the connectivity of the ligands is different in these complexes as the ligands are bonded to the metal center in *cis* configuration in **2**, while they are coordinated to the metal center in *trans* fashion in **3**. The Co−N bond distances in **2** and **3** lie within the range 1.9493(12)−1.963(2) Å, and the Co−O bond distances vary in between 1.8674(17)−1.9073(17) Å, which are again typical for the low spin cobalt(III) complexes.[41–43,58–63] In both complexes, the dioxolene C−O and C−C bond lengths are in the range 1.300(9)−1.3215(17) Å, and 1.408(3)−1.442(3) Å for **2** and **3** respectively, which are in-between the values reported for catecholate (1.33−1.39 Å) and semiquinonate (1.27−1.31 Å) ligands.[41–43,64–66] Moreover, the MOS values in **2** of –1.20 and –1.91 are apparent for the isolated semiquinone and catecholate ligands, respectively[47] and the MOS value is found to be –1.50 in **3**, suggesting the intermediate oxidation state of the *o*-dioxolene ligand in this complex.[67] The BVS values of **2** and **3** considering either the empirical bond parameters of Co(II) and Co(III) are found to be 3.17 and 3.22-3.23, respectively, further supporting the +III oxidation state of cobalt at room temperature in **2** and **3**. In summary, both complexes can be formulated as [ls-Co(III)(3,5-dbcat)(3,5-dbsq)] units with two ancillary aminopyridine ligands at the temperature of the data collection. Details structural analysis reveals that one hydrogen atom of the amine group from one of the coordinated 3-NH_2py ligands in **2** is engaged in hydrogen bonding interaction with one of the catecholate oxygen atoms from a neighboring molecule (N–H···O distance 3.149 Å) while the other hydrogen atom forms relatively stronger hydrogen bond with the oxygen atom of solvated DMF molecule with N–H···O distance 2.996 Å (Figure 5). The second 3-NH_2py ligand only establishes a N–H···π interaction with aromatic ring of the one of the dioxolene units as depicted in Figure 5. On the other hand, the symmetry equivalent 4-NH_2py ligands establish a well directional strong hydrogen bond with dimension N–H···O of 2.882 Å and the N–H···π (Figure 5) interaction in the solid state in **3**. Thus, different types of noncovalent interaction offered by the

aminopyridine isomers could be responsible of the isolation of *cis* and *trans* isomers of **2** and **3**, respectively, in the solid state.

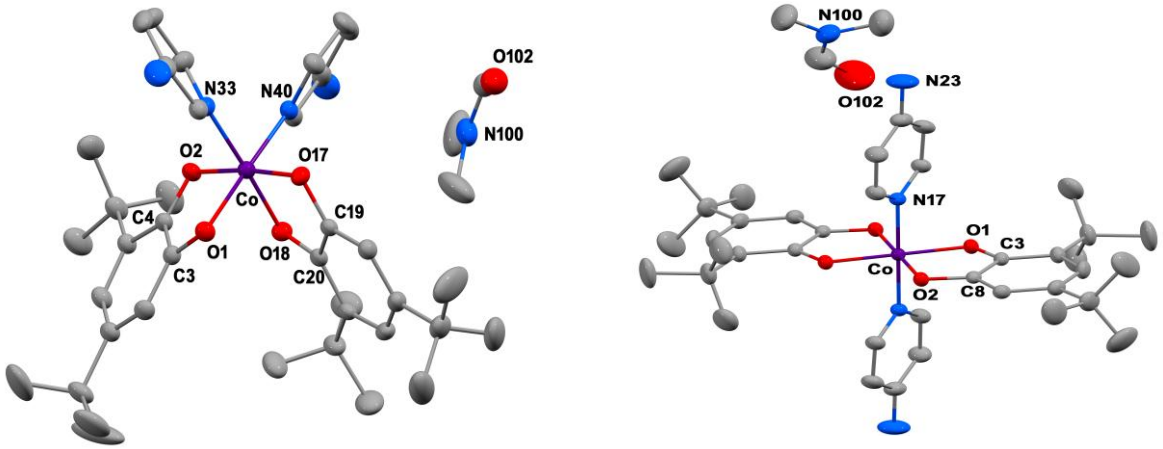

Figure 4. X-ray structures of **2** (left) and **3** (right) with partial atom numbering scheme. Ellipsoids are drawn at 30% probability. Hydrogen atoms are omitted for clarity.

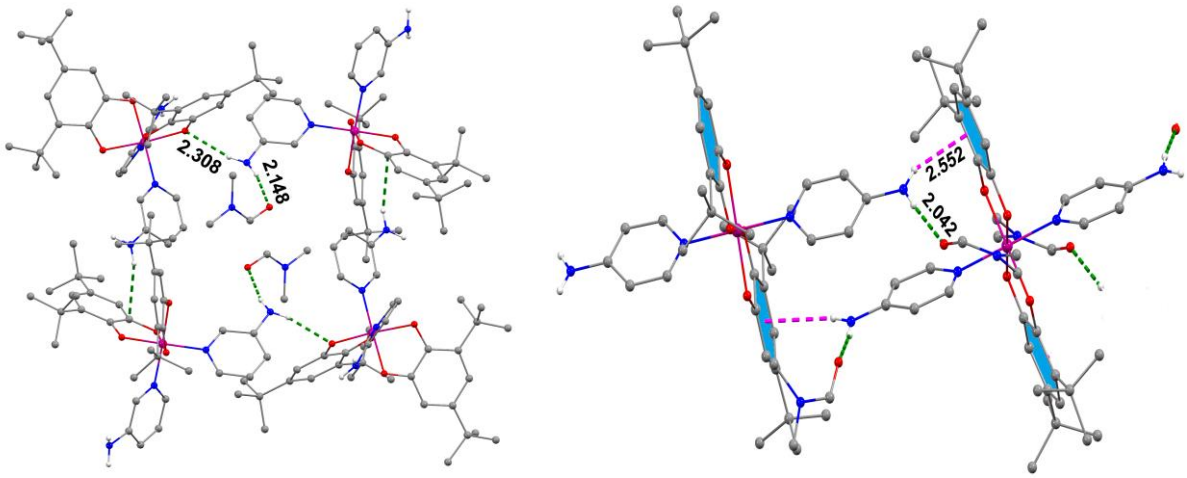

Figure 5. Molecular packing in **2** and **3** showing hydrogen bonding and N–H···π (for **3)** interactions.

Magnetic properties

The magnetic properties of **1**–**3** have been studied using a SQUID magnetometer working up to 380 K. The first measurements have been performed below 300 K to avoid the solvent loss

for the three compounds (Figure 6), and then cycles at higher temperatures (not more than 400 K) have been studied.

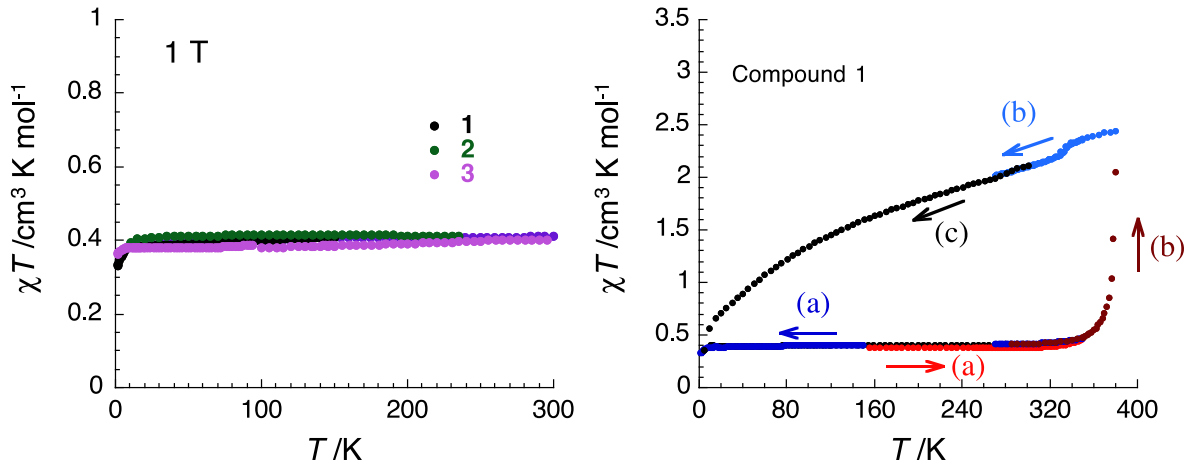

Figure 6. (left) Thermal variation of the χT products for **1**, **2** and **3** under a magnetic field of 1 T. (right) Thermal variation of the χT products for **1** under different temperature cycles. (a) 2 K-300 K (b) 150 K-380 K and (c) after immersion of the crystals (see text).

As shown in Figure 6, the three compounds exhibit similar magnetic properties below 300 K. They all have a χT product around 0.4 cm^3 mol^{-1} K at 300 K. This value is in agreement with the structural data of all three compounds that show discrete molecules of [Co^{III}(3,5-dbcat)(3,5-dbsq)$(L)_2$] where only the radical ligand 3,5-$dbsq^{\bullet-}$ has a spin equal to ½. Based on the TGA results these compounds are stable up to 380 K for **1** and **2** and 430 K for **3** (Figure S8) allowing a magnetic study up to 380 K, the maximum available temperature with our squid magnetometer. Although compounds **2** and **3** do not show significant modifications of their magnetic properties during a temperature cycle (heating 10–380 K and then cooling 380–10 K, Figure S9), compound **1** shows an intriguing behavior. When **1** is heated above 320 K, a sharp increase of the χT product is observed and a value of 2.4 cm^3 mol^{-1} K is obtained at 380 K suggesting that the compound is now in a high spin state. To understand the important magnetic changes of **1** upon heating, we have investigated further IR spectroscopic studies at room temperature of **1** after heating at 380 K. As shown in Figure 7, the catecholate bands of as synthesized complex **1** at *ca.* 1250–1300 cm^{-1} and 1480 cm^{-1} almost disappeared when the solid sample is heated at 380 K. On the other hand, the relative intensity of semiquinone bands at around 1440 and 1580 cm^{-1} increases significantly, which suggests the conversion of [Co(III)-(3,5-dbcat)(3,5-dbsq)] to [Co(II)-(3,5-dbsq)(3,5-dbsq)] as shown in equation 1.[20,43] The disappearance of acetonitrile CN stretching band at ca. 2248

cm^{-1} after the thermal heating (Figure S4) as well as about 5% mass loss up to 380 K in the thermo gravimetric studies which is equivalent to 92 % mass loss of lattice acetonitrile molecule, further indicating that the desolvation triggers valence tautomeric isomerism. As shown by the elemental analyses (Table S2) and IR spectroscopic studies, the desolvated species (**1**$_{\mathbf{heat380K}}$) does not include any more solvent even when it was kept under solvent vapour overnight. We have further carried out the PXRD studies, and from Figure S10, it is clear that the sample almost becomes amorphous when heated at 380 K and only a partial fraction of the pristine phase remained intact in this process. This result suggests that the crystal packing of the complex is almost destroyed after desolvation. Thus, this study overall suggests the thermally induced VT conversion of the complex in expense of an irreversible loss of the solvent molecules from the crystal lattice as shown in equation 1.

$$\underset{\mathbf{1}}{\textit{trans}\text{-}[Co^{III}(3,5\text{-dbcat})(3,5\text{-dbsq})(4\text{-Etpy})_2]\cdot CH_3CN} \xrightarrow[-CH_3CN]{380\ ^oC} \underset{\mathbf{1}_{\mathbf{heat380K}}}{\textit{trans}\text{-}[Co^{II}(3,5\text{-dbsq})_2(4\text{-Etpy})_2]} \qquad \text{Eq. 1}$$

From the above studies, it is now reasonable to consider that **1**$_{\mathbf{heat380K}}$ is a mixture of the pristine compound and a desolvated phase. When it is cooled, a small jump is observed around 330 K. This bump may come from a partial reverse thermal-induced valence tautomerism in the desolvated phase. Below 330 K, the χT product decreases monotonously to show a χT product of 2 cm^3 mol^{-1} K at 300 K. Finally, a third measurement has been performed after exposure of the heated crystals in a vial containing CH_3CN solvents to see if the initial state of **1** is reachable with this method. The resulted χT values (Figure 6, see cycle (c)) are very similar around room temperature to **1**$_{\mathbf{heat380K}}$ at the end of cycle (b). The immersed crystals of **1**$_{\mathbf{heat380K}}$ are not back in the initial isomer [Co^{III}(3,5-dbcat)(3,5-dbcat)(4-Etpy)$_2$] as stated earlier. Therefore, the observed magnetic behaviour for compound **1** is probably due to an irreversible valence tautomer induced by solvent loss. The EPR studies have also been performed to confirm the VT process in **1**. At room temperature, the signal of a radical with g = 2.00 could be detected, indicating the existence of a radical species, 3,5-dbsq$^{\bullet -}$, consistent with the crystal structure of the complex at room temperature. After the heating of the sample at 380 K to remove solvent acetonitrile molecules from the crystals, the EPR spectrum again recorded at room temperature that displays the stronger signal intensity (Figure 8), suggesting the increase of the magnetic signal through the desolvation induced valence tautomerism conversion from [Co^{III}(3,5-dbcat)(3,5-dbsq)(4-Etpy)$_2$] to [Co^{II}(3,5-dbcat)(3,5-dbcat)(4-Etpy)$_2$], consistent with the tendency observed in magnetic properties. In

contrast to compound **2** which shows rapid decomposition started from 383 K, compound **3** is stable at least up to 430 K as suggested by TGA data (Figure S8). We have therefore investigated the magnetic properties of **3** up to 430 K using a VSM magnetometer. Figure S11 shows the temperature dependence of the χT product of compound **3** during a temperature cycle between 150 K and 430 K (cooling and heating modes). Complex **3** shows an increase of its χT product from 0.4 cm^3 mol^{-1} K at 405 K to reach the value of 0.85 cm^3 mol^{-1} K at 430 K. Before the cooling, the sample is kept at this temperature and the χT product continues to increase to 1.12 cm^3 mol^{-1} K. This behavior is probably due to a progressive loss of the solvent molecules in the compound. During further cooling, a small decrease is observed and the χT product stays above 1 cm^3 mol^{-1} K, a value far from the theoretical value of 2.57 cm^3 mol^{-1} K for [Co(II)(3,5-dbsq)(3,5-dbsq)(4-Etpy)$_2$]. Finally compound **3** shows only a partial conversion towards the high spin isomer induced by solvent loss. In conclusion of the magnetic study, along this series of compounds, compound **1** has the most interesting magnetic behavior. The solvated form of **1** has a low spin configuration in agreement with the low-spin valence isomer [Co(III)(3,5-dbcat)(3,5-dbsq)(4-Etpy)$_2$].CH_3CN. When heated above 340 K, a simultaneous solvent loss and a valence tautomerism occur to stabilize the high-spin valence isomer [Co(II)(3,5-dbsq)(3,5-dbsq)(4-Etpy)$_2$] at 380 K.

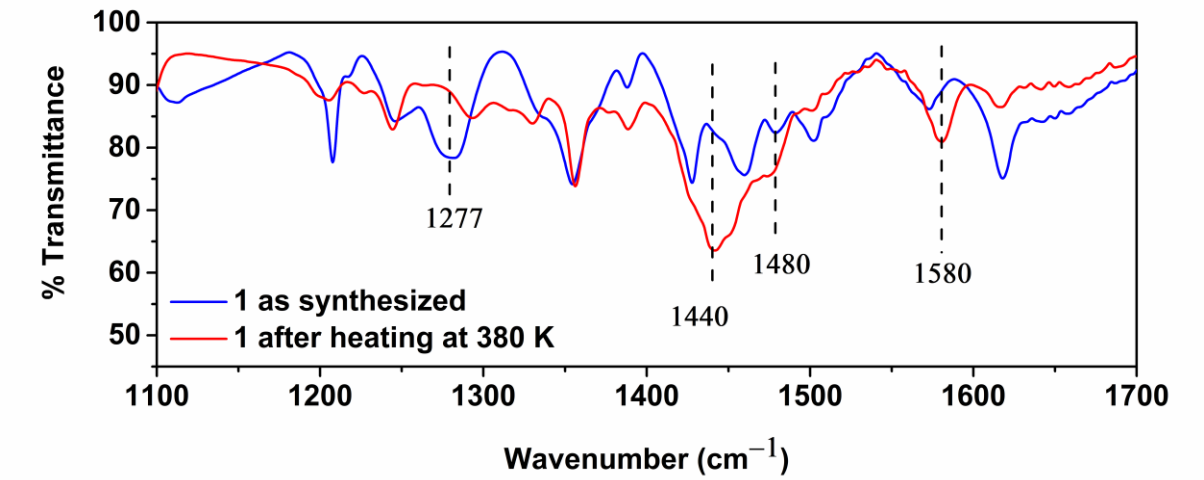

Figure 7. ATR-IR spectra of as synthesized complex **1** and after heating at 380 K.

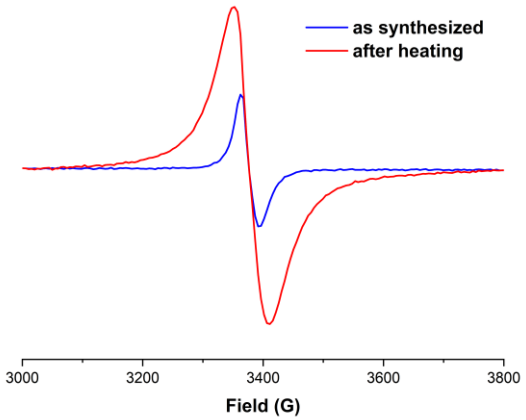

Figure 8. EPR spectra of **1** as from synthesized (blue) and after heating at 380 K (red) (frequency: 9.44 GHz; modulation: 1.0 mT; power: 0.711 mW).

Optical reflectivity

Some complexes based on Co ion, 3,5-dbcat^{2-} and 3,5-dbsq$^{\bullet-}$ ligands are known to exhibit photo-induced properties[41,42,70,71] that correspond to a photo-induced valence tautomerism. These photo-induced can be followed by optical and/or magnetic measurements because the two valence isomers present distinct optical and magnetic properties. To check if our compounds show such properties, we have used optical reflectivity to measure photo-induced optical properties. We have selected compound **1** because it shows the most complete conversion from one state to the other one. The optical reflectivity spectra of **1** and **1** after heating at 380 K (noted here after $\mathbf{1}_{\mathbf{heat380}}$) are shown on Figure S12 and Figure 9. **1** and $\mathbf{1}_{\mathbf{heat380}}$ exhibit different spectra in agreement with the nature of their valence states. We have then measured the wavelength dependence using a set of 14 LEDs (working between 1100 nm to 365 nm with a power of 2 mW/cm^2) on the optical spectra for **1** and $\mathbf{1}_{\mathbf{heat380}}$ (Figure S13)**.** Where as $\mathbf{1}_{\mathbf{heat380}}$ does not present significant modifications, **1** shows a small photoactivity in the visible range. An additional measurement has been done for **1** using a 405-nm LED with a power of 10mW/cm^2. Even in these conditions, the photo-induced modifications remain small (Figure S14) meaning that the measured photoactivity of **1** is probably a surface effect.

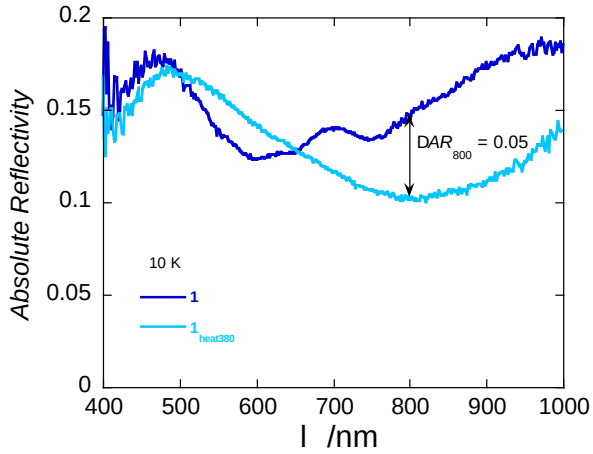

Figure 9. Optical reflectivity spectra at 10 K for compound **1 (**in the pristine form) and in $\mathbf{1}_{\mathbf{heat380}}$ (**1** after heating at 380 K).

CONCLUSIONS

We have synthesized and characterized three new cobalt-dioxolene complexes (**1–3**) using three different ancillary pyridine derivatives. All these complexes are thermodynamically controlled products and crystallized as *cis* isomer (**2**) and *trans* isomers (**1** and **3)**. X-ray diffraction data for all compounds at room temperature suggest Co(III)(3,5-dbcat)(3,5-dbsq) charge distribution in the solid state. Interestingly, in an identical reaction condition using positional isomers of aminopyridine (3-aminopyridine for **2**, and 4-aminopyridine for **3**), we have been able to isolate the *cis* and *trans* isomers in cobalt-dioxolene chemistry. Exploration of the crystal structures reveal that pendent amine groups of the pyridyl ligands establish different non-covalent interactions in the solid state that play crucial role in the isolation of the *cis* and *trans* geometrical isomers for the first time in cobalt-dioxolene chemistry induced by the positional isomers of the ancillary ligands as only variable. Temperature dependence of magnetic susceptibility data for all compounds between 2 and 300 K are consistent with the structural studies. When the samples were heated above room temperature, complex **1** exhibits almost a full VT interconversion from low spin Co(III)-(3,5-dbcat)(3,5-dbsq) to high spin Co(II)-(3,5-dbsq)(3,5-dbsq) species, while a partial interconversion observed for complex **3** even heating up to 430 K. The observed magnetic behavior for these compounds is probably due to an irreversible valence tautomerism induced by the progressive loss of lattice solvent molecules. Photoactivity of complex **1** in the visible region is small that probably comes from a surface effect.

ASSOCIATED CONTENT

Supporting Information

The Supporting Information is available free of charge at https://pubs.acs.org/doi:

Supplementary data including bond angles, IR and UV-vis spectral data, cyclic voltammogram, EPR spectral data, magnetic measurements and optical reflectivity studies.

Accession Codes

CCDC 2073857-2073859 for **1–3** contain the supplementary crystallographic data for this paper. These data can be obtained free of charge via www.ccdc.cam.ac.uk/data_request/cif, or by emailing data_request@ccdc.cam.ac.uk, or by contacting The Cambridge Crystallographic Data Centre, 12 Union Road, Cambridge CB2 1EZ, UK; fax: +44 1223 336033.

AUTHOR INFORMATION

Corresponding Author

Anangamohan Panja, Department of Chemistry, Panskura Banamali College, Panskura RS, WB 721152; Department of Chemistry, Gokhale Memorial Girls' College, 1/1 Harish Mukherjee Road, Kolkata-700020, India**.** E-mail: ampanja@yahoo.co.in

Corine Mathonière, Univ. Bordeaux, CNRS, Bordeaux INP, ICMCB, UMR 5026, F-33600 Pessac, France; Univ. Bordeaux, CNRS, Centre de Recherche Paul Pascal, CRPP, UMR 5031, F-33600 Pessac, France. E-mail: corine.mathoniere@u-bordeaux.fr

Author Contributions

The manuscript was written through contributions of all authors. All authors have given approval to the final version of the manuscript.

Notes

There are no conflicts to declare.

ACKNOWLEDGMENT

A.P. thanks the Department of Science and Technology (DST), New Delhi, India, under FAST Track Scheme (Order SB/FT/CS-016/2012) for financial support. X.Q. thanks the CSC for PhD funding. C.M. acknowledges the Financial support from the CNRS (Pessac,) and the University of Bordeaux.

ABBREVIATIONS

3,5-dbcat^{2-}, 3,5-di-*tert*-butyl-catacholate; 3,5-dbsq$^{\bullet-}$, 3,5-di-*tert*-butyl-semiquinonate; 4-Etpy, 4-ethylpyridine; 3-NH_2py, 3-aminopyridine; 4-NH_2py, 4-aminopyridine; DMF, N,N-dimethylformamide.

REFERENCES

(1) Kumar K. S.; Ruben, M. Emerging trends in spin crossover (SCO) based functional materials and devices. *Coord. Chem. Rev*. **2017**, *346*, 176–205.

(2) Sato, O. Dynamic molecular crystals with switchable physical properties. *Nat. Chem*. **2016**, *8*, 644–656.

(3) Calzolari, A.; Chen, Y.; Lewis, G. F.; Dougherty, D. B.; Shultz D.; Nardelli, M. B. Complex Materials for Molecular Spintronics Applications: Cobalt Bis(dioxolene) Valence Tautomers, from Molecules to Polymers**.** *J. Phys. Chem. B*, **2012**, *116*, 13141–13148.

(4) Dei A.; Sorace, L. Cobalt-Dioxolene Redox Isomers: Potential Spintronic Devices**.** *Appl. Magn. Reson*. **2010**, *38*, 139–153.

(5) Sedo, J.; Saiz-Poseu, J.; Busque F.; Ruiz-Molina, D. Catechol‐Based Biomimetic Functional Materials. *Adv. Mater*. **2013**, *25*, 653–701.

(6) Wang, M.; Li, Z.Y.; Ishikawa R.; Yamashita, M. Spin crossover and valence tautomerism conductors**.** *Coord. Chem. Rev.* **2021**, *435*, 213819.

(7) Rajput, A.; Sharma, A.K.; Barman, S.K.; Saha A.; Mukherjee, R. Valence tautomerism and delocalization in transition metal complexes of *o*-amidophenolates and other redox-active ligands. Some recent results**.** *Coord. Chem. Rev.* **2020**, *414*, 213240.

(8) Ferrando-Soria, J.; Vallejo, J.; Castellano, M.; Martinez-Lillo, J.; Pardo, E.; Cano, J.; Castro, I.; Lloret, F.; Ruiz-Garcia R.; Julve, M. Molecular magnetism, *quo vadis?* A historical perspective from a coordination chemist viewpoint. *Coord. Chem. Rev.* **2017**, *339*, 17–103.

(9) Létard, J.-F.; Guionneau P.; Goux-Capes, L. *Towards Spin Crossover Applications. In Spin Crossover in Transition Metal Compounds;* Springer: Berlin, Germany, **2004**, *235*, 221−249.

(10) Sato, O.; Tao J.; Zhang, Y.-Z. Control of Magnetic Properties through External Stimuli. *Angew. Chem., Int. Ed.* **2007**, *46*, 2152–2187.

(11) Hendrickson D. N.; Pierpont, C. G. Valence Tautomeric Transition Metal Complexes. *Top. Curr. Chem*. **2004**, *234*, 63–95.

(12) Dei, A.; Gatteschi, D.; Sangregorio C.; Sorace, L. Quinonoid Metal Complexes: Toward Molecular Switches. *Acc. Chem. Res.* **2004**, *37*, 827– 835.

(13) Evangelio E.; Ruiz-Molina, D. Valence Tautomerism: New Challenges for Electroactive Ligands. *Eur. J. Inorg. Chem*. **2005**, *15*, 2957–2971.

(14) Nadurata V.L.; Boskovic, C. Switching metal complexes *via* intramolecular electron transfer: connections with solvatochromism. *Inorg. Chem. Front.* **2021**, *8*, 1840-1864.

(15) Li, D.; Clérac, R.; Roubeau, O.; Harté, E.; Mathonière, C.; Le Bris R.; Holmes, S. M. Magnetic and Optical Bistability Driven by Thermally and Photoinduced Intramolecular Electron Transfer in a Molecular Cobalt−Iron Prussian Blue Analogue. *J. Am. Chem. Soc.* **2008**, *130*, 252–258.

(16) Aguilà, D.; Prado, Y.; Koumousi, E. S.; Mathonière C.; Clérac, R. Switchable Fe/Co Prussian blue networks and molecular analogues. *Chem. Soc. Rev*. **2016**, *45*, 203–224.

(17) Mathonière, C. Metal-to-Metal Electron Transfer: A Powerful Tool for the Design of Switchable Coordination Compounds. *Eur. J. Inorg. Chem*. **2018**, 248–258

(18) Tezgerevska, T.; Alley K. G.; Boskovic, C. Valence tautomerism in metal complexes: Stimulated and reversible intramolecular electron transfer between metal centers and organic ligands. *Coord. Chem. Rev*. **2014**, *268*, 23–40.

(19) Fleming, C.; Chung, D.; Ponce, S.; Brook, D. J. R.; DaRos, J.; Das, R.; Ozarowski A.; Stoian, S. A. Valence tautomerism in a cobalt-verdazyl coordination compound. *Chem. Commun*. **2020**, *56*, 4400–4403

(20) Li, B.; Wang, X.-N.; Kirchon, A.; Qin, J.-S.; Pang, J.-D.; Zhuang, G.-L.; Zhou, H.-C. Sophisticated Construction of Electronically Labile Materials: A Neutral, Radical-Rich, Cobalt Valence Tautomeric Triangle. *J. Am. Chem. Soc*. **2018**, *140*, 14581–14585.

(21) Boskovic, C. *Valence Tautomeric Transitions in Cobalt-dioxolene Complexes, in Spin-Crossover Materials*; Halcrow, M. A., Ed.; John Wiley & Sons Ltd: Chichester, **2013**, 203−224.

(22) Gransbury, G. K.; Boulon, M.-E.; Petrie, S.; Gable, R. W.; Mulder, R. J.; Sorace, L.; Stranger R.; Boskovic, C. DFT Prediction and Experimental Investigation of Valence Tautomerism in Cobalt-Dioxolene Complexes. *Inorg. Chem*. **2019**, *58*, 4230–4243

(23) Tezgerevska, T.; Rousset, E.; Gable, R. W.; Jameson, G. N. L.; Sañudo, E. C.; Starikova A.; Boskovic, C. Valence tautomerism and spin crossover in pyridinophane–cobalt–dioxolene complexes: an experimental and computational study. *Dalton Trans*. **2019**, *48*,

11674–11689.

(24) Drath, O.; Gable, R. W.; Poneti, G.; Sorace L.; Boskovic, C. One Dimensional Chain and Ribbon Cobalt–Dioxolene Coordination Polymers: A New Valence Tautomeric Compound. *Cryst. Growth Des*. **2017**, *17*, 3156–3162.

(25) Drath, O.; Gable, R. W.; Moubaraki, B.; Murray, K. S.; Poneti, G.; Sorace L.; Boskovic, C. Valence Tautomerism in One-Dimensional Coordination Polymers. *Inorg. Chem*. **2016**, *55*, 4141–4151.

(26) Beni, A.; Dei, A.; Laschi, S.; Rizzitano M.; Sorace, L. Tuning the Charge Distribution and Photoswitchable Properties of Cobalt–Dioxolene Complexes by Using Molecular Techniques. *Chem.- Eur. J*. **2008**, *14*, 1804−1813.

(27) Pour, Y.S.; Safaei, E.; Wojtczak, A.; Jagličić, Z. Valence tautomerism in catecholato cobalt Bis(phenolate) diamine complexes as models for Enzyme–substrate adducts of catechol dioxygenases. *Polyhedron*, **2020**, *187*, 114620.

(28) Wu, S.-Q.; Liu, M.; Gao, K.; Kanegawa, S.; Horie, Y.; Aoyama, G.; Okajima, H.; Sakamoto, A.; Baker, M. L.; Huzan, M. S.; Bencok, P.; Abe, T.; Shiota, Y.; Yoshizawa, K.; Xu, W.; Kou H.-Z.; Sato, O. Macroscopic Polarization Change via Electron Transfer in a Valence Tautomeric Cobalt Complex. *Nat. Commun*. **2020**, *11*, 1992.

(29) Alley, K. G.; Poneti, G.; Robinson, P. S. D.; Nafady, A.; Moubaraki, B.; Aitken, J. B.; Drew, S. C.; Ritchie, C.; Abrahams, B. F.; Hocking, R. K.; Murray, K. S.; Bond, A. M.; Harris, H. H.; Sorace L.; Boskovic, C. Redox Activity and Two-Step Valence Tautomerism in a Family of Dinuclear Cobalt Complexes with a Spiroconjugated Bis(dioxolene) Ligand. *J. Am. Chem. Soc*. **2013**, *135*, 8304–8323.

(30) Bubnov, M. P.; Skorodumova, N. A.; Arapova, A. V.; Smirnova, N. N.; Samsonov, M. A.; Fukin, G. K.; Cherkasov V. K.; Abakumov, G. A. Lattice-Modulated Phase Transition Coupled with Redox-Isomeric Interconversion of *o*-Semiquinone–Catecholato into Bis(*o*-semiquinonato) Cobalt Complexes. *Inorg. Chem*. **2015**, *54*, 7767–7773.

(31) Kanegawa, S.; Kang S.; Sato, O. Preparation and Valence Tautomeric Behavior of a Cobalt–Dioxolene Complex with a New TTF-functionalized Phenanthroline Ligand. *Chem. Lett.* **2013**, *42*, 700–702.

(32) Dai, J.; Kanegawa, S.; Li, Z.; Kang S.; Sato, O. A Switchable Complex Ligand Exhibiting Photoinduced Valence Tautomerism. *Eur. J. Inorg. Chem*. **2013**, 4150–4153.

(33) Ribeiro, M. A.; Lanznaster, M.; Silva, M. M. P.; Resende, J. A. L. C.; Pinheiro, M. V.

B.; Krambrock, K.; Stumpf H. O.; Pinheiro, C. B. Cobalt lawsone complexes: searching for new valence tautomers. *Dalton Trans*. **2013**, *42*, 5462–5470.

(34) Gransbury, G. K.; Livesay, B. N.; Janetzki, J. T.; Hay, M. A.; Gable, R. W.; Shores, M. P.; Starikova A.; Boskovic, C. Understanding the Origin of One- or Two-Step Valence Tautomeric Transitions in Bis(dioxolene)-Bridged Dinuclear Cobalt Complexes. *J. Am. Chem. Soc*. **2020**, *142*, 10692–10704.

(35) Roux, C.; Adams, D. M.; Itie´, J.-P.; Polian, A.; Hendrickson D. N.; Verdaguer, M. Pressure-Induced Valence Tautomerism in Cobalt *o*-Quinone Complexes: An X-ray Absorption Study of the Low-Spin [Co^{III}(3,5-DTBSQ)(3,5-DTBCat)(phen)] to High-Spin [Co^{II}(3,5-DTBSQ)$_2$(phen)] Interconversion. *Inorg. Chem*. **1996**, *35*, 2846–2852.

(36) Poneti, G.; Mannini, M.; Sorace, L.; Sainctavit, P.; Arrio, M.-A.; Otero, E.; Cezar J. C.; Dei, A. Soft‐X‐ray‐Induced Redox Isomerism in a Cobalt Dioxolene Complex. *Angew. Chem., Int. Ed*. **2010**, *49*, 1954–1957

(37) Liang, H. W.; Kroll, T.; Nordlund, D.; Weng, T.-C.; Sokaras, D.; Pierpont C. G.; Gaffney, K. J. Charge and Spin-State Characterization of Cobalt Bis(*o*-dioxolene) Valence Tautomers Using Co Kβ X-ray Emission and L-Edge X-ray Absorption Spectroscopies. *Inorg. Chem.* **2017**, *56*, 737–747

(38) Francisco, T. M.; Gee, W. J.; Shepherd, H. J.; Warren, M. R.; Shultz, D. A.; Raithby P. R.; Pinheiro, C. B. Hard X-ray-Induced Valence Tautomeric Interconversion in Cobalt-*o*-Dioxolene Complexes. *J. Phys. Chem. Lett*. **2017**, *8*, 4774–4778.

(39) Markevtsev, I. N.; Monakhov, M. P.; Platonov, V. V.; Mischenko, A. S.; Zvezdin, A. K.; Bubnov, M. P.; Abakumov G. A.; Cherkasov, V. K. Field-induced spin phase transition in a Co complex. *J. Magn. Magn. Mater*. **2006**, *300*, 407–410

(40) Buchanan R. M.; Pierpont, C. G. Tautomeric catecholate-semiquinone interconversion via metal-ligand electron transfer. Structural, spectral, and magnetic properties of (3,5-di-tert-butylcatecholato)(3,5-di-tert-butylsemiquinone)(bipyridyl)cobalt(III), a complex containing mixed-valence organic ligands. *J. Am. Chem. Soc*. **1980**, *102*, 4951–4957.

(41) Schmidt, R. D.; Shultz, D. A.; Martin J. D.; Boyle, P. D. Goldilocks Effect in Magnetic Bistability: Remote Substituent Modulation and Lattice Control of Photoinduced Valence Tautomerism and Light-Induced Thermal Hysteresis. *J. Am. Chem. Soc*. **2010**, *132,* 6261–6273.

(42) Schmidt, R. D.; Shultz D. A.; Martin, J. D. Magnetic Bistability in a Cobalt Bis(dioxolene) Complex: Long-Lived Photoinduced Valence Tautomerism. *Inorg.*

Chem. **2010**, *49*, 3162–3168.

(43) Mulyana, Y.; Poneti, G.; Moubaraki, B.; Murray, K. S.; Abrahams, B. F.; Sorace L.; Boskovic, C. Solvation effects on the valence tautomeric transition of a cobalt complex in the solid state. *Dalton Trans*. **2010**, *39*, 4757– 4767.

(44) Panja, A.; Jana, N. C.; Bauzá, A.; Frontera A.; Mathonière, C. Solvent-Triggered Cis/Trans Isomerism in Cobalt Dioxolene Chemistry: Distinguishing Effects of Packing on Valence Tautomerism. *Inorg. Chem.* **2016**, *55*, 8331–8340.

(45) Panja, A. Unusual structural features in tetrabromocatechol-chelated dinuclear manganese(III) complex: Synthesis, electrochemistry and thermally induced valence tautomerism. *Inorg. Chem. Commun.* **2012**, *24*, 140–143

(46) Panja. A. A series of tetrabromocatecholate chelated cobalt(III) complexes with various N-donor ancillary ligands: syntheses, crystal structures, co-crystallization, thermally induced valence tautomerism and electrochemical studies. *RSC Adv.* **2013**, *3*, 4954–4963.

(47) Panja, A.; Jana, N. C.; Patra, M.; Brandão, P.; Moore, C. E.; Eichhorn D. M.; Frontera, A. Valence tautomerism induced nucleophilic ipso substitution in a coordinated tetrabromocatecholate ligand and diverse catalytic activity mimicking the function of phenoxazinone synthase. *J. Mol. Catal. A.* **2016**, *412*, 56–66

(48) Jana, N. C.; Brandão P.; Panja, A. Tuning the geometry and biomimetic catalytic activity of manganese(III)-tetrabromocatecholate based robust platforms by introducing substitution at pyridine. *J. Inorg. Biochem.* **2016**, *159*, 96–106

(49) Jana, N. C.; Brandão, P.; Bauzá, A.; Frontera A.; Panja, A. Influence of ancillary ligands on preferential geometry and biomimetic catalytic activity in manganese(III)-catecholate systems: A combined experimental and theoretical study. *J. Inorg. Biochem*. **2017**, *176*, 77–89

(50) Panja, A.; Jana, N. C.; Bauzá, A.; Adak, S.; Mwania, T. M.; Eichhorn D. M.; Frontera, A. Introducing Supramolecular Interactions into Robust Bis(tetrabromocatecholate) Chelated Manganese(III) Systems and Biomimetic Catalytic Activity. *ChemistrySelect,* **2017**, *2*, 2094–2105

(51) Panja, A.; Jana, N. C.; Adak S.; Pramanik, K. Insight into the origin of catechol oxidase activity in a rare Mn^{II}/Mn^{III} mixed valence ion pair complex: An account of comparative biomimetic catalytic study. *Inorg. Chim. Acta*, **2017**, *459*, 113– 123.

(52) Panja A.; Frontera, A. Valence‐Tautomerism‐Driven Aromatic Nucleophilic

Substitution in Cobalt‐Bound Tetrabromocatecholate Ligands – Influence of Positive Charge at the Ligand Backbone on Phenoxazinone Synthase Activity. *Eur. J. Inorg. Chem.* **2018***, 7*, 924–931.

(53) Sheldrick, G. M. SADABS, University of Göttingen, Germany, **1996**.

(54) Sheldrick, G. M. *Acta Crystallogr., Sect. A: Found. Crystallogr*., **2008**, *64*, 112.

(55) Janetzki, J. T., Zahir, F. Z. M., Gable, R. W., Phonsri, W., Murray, K. S., Goerigk, L., Boskovic, C. A Convenient DFT-Based Strategy for Predicting Transition Temperatures of Valence Tautomeric Molecular Switches. *Inorg. Chem*. **2021**, *60*, 14475−14487

(56) Adams, D. M.; Dei, A.; Rheingold A. L.; Hendrickson, D. N. Bistability in the [CoII(semiquinonate)2] to [CoIII(catecholate)(semiquinonate)] valence-tautomeric conversion. *J. Am. Chem. Soc*. **1993**, *115*, 8221– 8229

(57) Lynch, M.W.; Valentine M.; Hendrickson, D. N. Mixed-valence semiquinone-catecholate-iron complexes. *J. Am. Chem. Soc.* **1982**, *104*, 6982–6989.

(58) Pierpont C. G.; Buchanan, R. M. Transition metal complexes of o_benzoquinone, o-semiquinone, and catecholate ligands. *Coord. Chem. Rev.* **1981**, *38*, 45–87

(59) Pierpont C. G.; Lange, C. W. The chemistry of transition metal complexes containing catechol and semiquinone ligands. *Prog. Inorg. Chem.* **1994**, *41*, 331–442.

(60) Verani, C. N.; Gallert, S.; Bill, E.; Weyhermüller, T.; Wieghardt K.; Chaudhuri, P. [Tris(*o*-iminosemiquinone)cobalt(III)]–a radical complex with an $S_t = {}^3/_2$ ground state. *Chem. Commun.* **1999**, 1747–1748

(61) Chaudhuri, P.; Bill, E.; Wagner, R.; Pieper, U.; Biswas B.; Weyhermüller, T. Radical−Ligand-Derived C−N Coupling, Ga(III)−Radical vs Low-Spin Co(III)−Radical Reactivity. *Inorg. Chem*. **2008**, *47*, 5549–5551.

(62) Chakraborty, B.; Ghosh, I.; Jana R. D.; Paine, T. K. Oxidative C–N bond cleavage of (2-pyridylmethyl)amine-based tetradentate supporting ligands in ternary cobalt(II)–carboxylate complexes. *Dalton Trans*. **2020**, *49*, 3463–3472.

(63) Li, B.; Chen, L.; Wei, R.; Tao, J.; Huang, R.; Zheng L.; Zheng, Z. Thermally Induced and Photoinduced Valence Tautomerism in a Two-Dimensional Coordination Polymer. *Inorg. Chem*. **2011**, *50*, 424–426.

(64) Adams D. M.; Hendrickson, D. N. Pulsed Laser Photolysis and Thermodynamics Studies of Intramolecular Electron Transfer in Valence Tautomeric Cobalt *o*-Quinone Complexes. *J. Am. Chem. Soc*. **1996**, *118*, 11515–11528

(65) Paquette, M. M.; Plaul, D.; Kurimoto, A.; Patrick B. O.; Frank, N. L. Opto-Spintronics:

Photoisomerization-Induced Spin State Switching at 300 K in Photochrome Cobalt–Dioxolene Thin Films. *J. Am. Chem. Soc*. **2018**, *140*, 14990–15000

(66) Mörtel, M.; Seller, M.; Heinemann F. W.; Khusniyarov, M. M. A valence tautomeric cobalt–dioxolene complex with an anchoring group for prospective chemical grafting to metal oxides. *Dalton Trans.* **2020**, *49*, 17532–17536.

(67) Brown, S. N. Metrical Oxidation States of 2-Amidophenoxide and Catecholate Ligands: Structural Signatures of Metal–Ligand π Bonding in Potentially Noninnocent Ligands. *Inorg. Chem*. **2012**, *51*, 1251–1260.

(68) Brown, I. D.; Altermatt, D. Bond-Valence Parameters Obtained from a Systematic Analysis of the Inorganic Crystal Structure Database. *Acta Crystallogr. B*. **1985**, B41, 244.

(69) Brown, I. D. Chemical and Steric Constraints in Inorganic Solids. *Acta Crystallogr. B*. **1992**, B48, 553.

(70) Sato O.; Cui, A. Photo-induced Valence Tautomerism in Co Complexes. *Acc. Chem. Res*. **2007**, ***40***, 361–369

(71) Beni, A.; Dei, A.; Rizzitano M.; Sorace, L. Unprecedented optically induced long-lived intramolecular electron transfer in cobalt–dioxolene complexes. *Chem. Commun.* **2007**, 2160–2162.

For Table of Contents Use Only

Impact of Positional Isomers on the Selective Isolation of cis-trans Isomers in Cobalt-dioxolene Chemistry and Solvation Effects on the Valence Tautomerism in the Solid State

Narayan Ch. Jana, Xing-Hui Qi, Paula Brandão, Corine Mathonière, and Anangamohan Panja

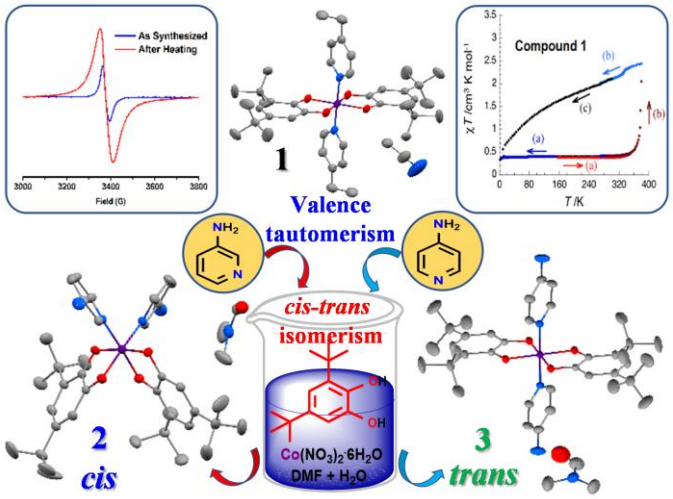

Influence of positional isomers of aminopyridine on the selective isolation of cis-trans isomers in cobalt-dioxolene chemistry and effect of solvation on valence tautomerism have been explored.